The Effect of Surfactants on the Flow Characteristics of Falling Liquid Films

W. J. STROBEL and STEPHEN WHITAKER

University of California, Davis, California

Experimental values of the wave length and wave velocity have been obtained for dilute solutions of valeric and hexanoic acid for a vertical falling liquid film. The wave length was unaffected by the surfactants for Reynolds numbers in the range 5 to 100; however, the wave velocity was decreased for increased surface concentrations of the two acids. This is in direct contradiction to previous theoretical work, and the explanation for the anomaly is that the free surface velocity is greatly retarded by the adsorption of the surface active agents.
In an effort to determine the extent of this retardation, an approximate form of the diffusion equation and the equations of motion were solved subject to boundary conditions describing the effect of the adsorbed surfactant on the surface stress. The results indicate that the entrance length can be increased several orders of magnitude by the addition of small amounts of surfactant.

The flow characteristics of falling liquid films have been a subject of interest in connection with gas absorption studies (*9, 17, 24, 27*) primarily because the falling film appears to provide a reasonably well defined interfacial area and contact time. Knowledge of the nature of the flow of thin liquid films is also of importance in analyzing heat transfer rates for ablating space vehicles (*31*), in the design of cooling systems for high temperature turbine blades (*15*), and in the analysis of mass transfer rates in certain desalinization processes (*6*).

By itself, the falling liquid film provides a reasonable experimental tool for studying the effect of surface active agents on bulk fluid motion. In addition to the wave length and wave velocity, one can also observe the location (measured from the top of the film) of the first visible waves as a function of Reynolds number, and the rate of approach of the surface velocity to the value predicted for uniform flow.

In order to test recent mathematical studies (*1, 4, 28, 29*) of the stability of vertical falling liquid films, an experimental study of the wave length and wave velocity was planned. In a sense, the experimental study was unsuccessful for the data were obtained under conditions which did not allow the direct comparison of theory and experiment; however, some interesting characteristics of the flow were observed and analyzed, and it seems appropriate to report the results at this time.

EXPERIMENTAL METHOD

The experimental method used in this study is essentially identical to that used by Jones (*13*) and described elsewhere (*14*). A schematic representation of the experimental equipment is shown in Figure 1. Two parallel beams of light pass through holes of diameter 0.08 cm., and are directed at the film at two points 1.27 cm. apart. As the light passes through the wavy film, the beam is refracted and strikes the cathode of a photomultiplier tube at a position which depends on the slope of the gas-liquid interface. Since the sensitivity (or amplification factor) of the cathode of a photomultiplier tube is never uniform the varying position at which the light beam strikes the cathode gives rise to a varying output from the tube. In this method one obtains two signals which are proportional to the slopes of the gas-liquid interface at two points 1.27 cm. apart, and from these two signals the wave length and wave velocity can be determined (*14*). A severe restriction of this experimental set up was that measurements could be made only over the top 11 cm. of the column.

EXPERIMENTAL RESULTS

The measured wave numbers for pure water are compared with previous experimental data (*14, 25*) and theoretical results (*2, 28*) in Figure 2. Both the theoretical analysis and the interpretation of the experimental data are based on the assumption that the primary or undisturbed flow is described by

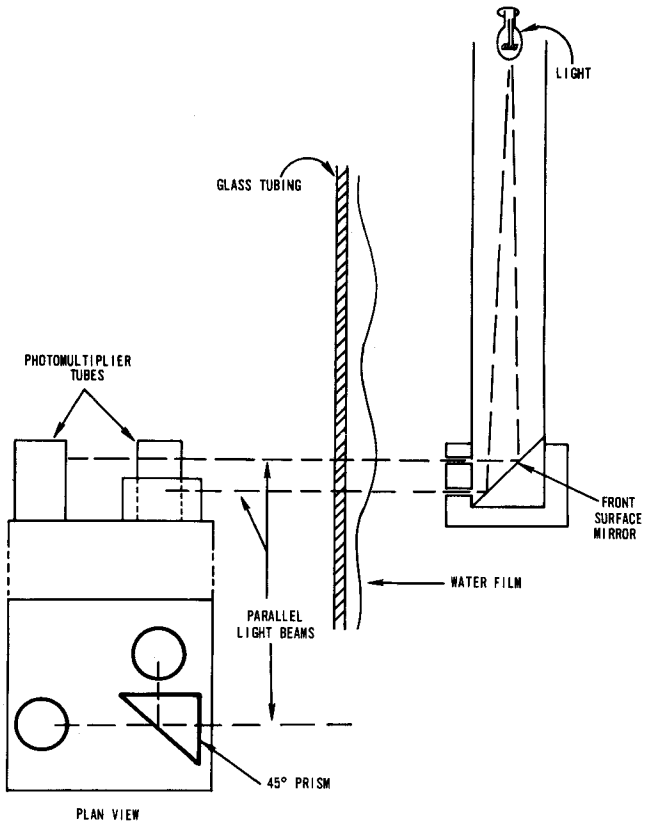

Fig. 1. Experimental system.

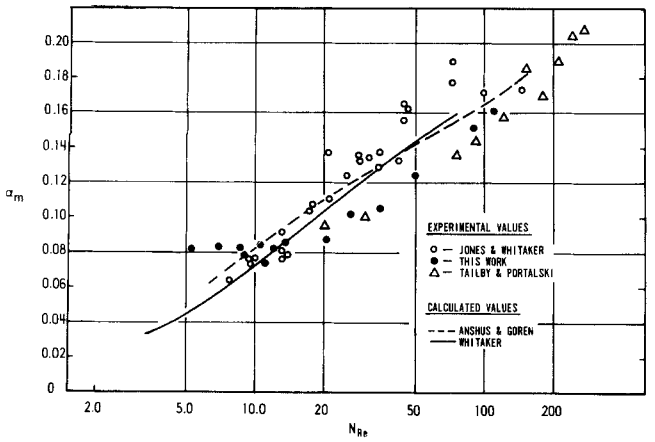

Fig. 2. Wave number having maximum growth rate vs. Reynolds number.

$$u = u_o\left[1 - \left(\frac{y}{h}\right)^2\right] \tag{1}$$

where u is the velocity, y is measured from the free surface, and h is the film thickness. The free surface velocity u_o may be represented as

$$u_o = gh^2/2\nu \tag{2}$$

and the Reynolds number is defined as

$$N_{Re} = u_o h/\nu \tag{3}$$

The experimental studies lead to the determination of a wave velocity c_r and a wave length λ. These quantities are generally represented in terms of a dimensionless wave velocity C_r defined by

$$C_r = c_r/u_o \tag{4}$$

and a dimensionless wave number given by

$$\alpha = 2\pi h/\lambda \tag{5}$$

The results shown in Figure 2 for the measured wave number indicate reasonable agreement with previous work with the exception of those values for Reynolds numbers less than 10. Similar agreement is illustrated in Figure 3 where the dimensionless wave velocity is compared with previous experimental (*14*) and theoretical work (*2, 28*). The existence of measured values of C_r greater than 2.0 for $N_{Re} < 10$ indicates that there is considerable error in the measurements in the low Reynolds number region.

EFFECT OF SURFACTANTS

It was decided in this study to examine the effect of four straight chain aliphatic acids on the wave structure of

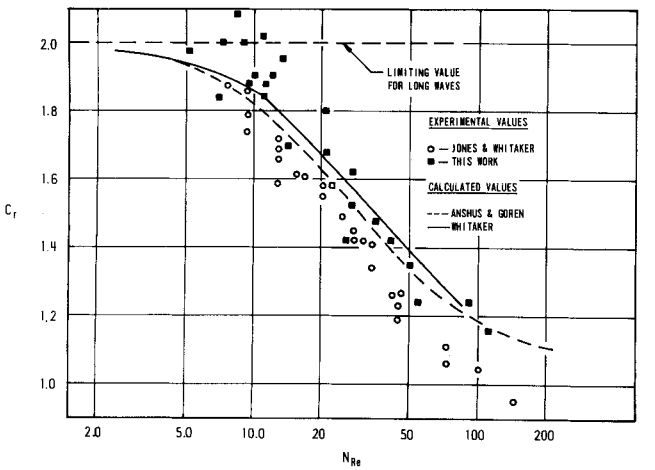

Fig. 3. Wave velocity for most unstable wave vs. Reynolds number.

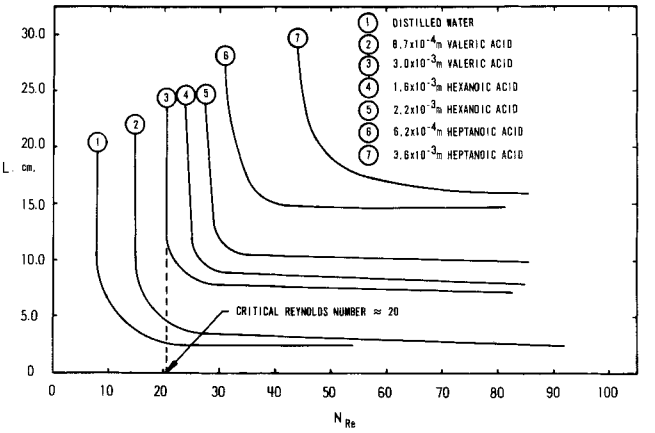

Fig. 4. Distance at which waves become visible vs. Reynolds number.

water films. These acids were reagent grade chemicals. The four acids were valeric (boiling point 186 to 187°C), hexanoic (melting point −5 to −3°C), heptanoic (melting point −8 to −6°C), and octanoic (melting point 15 to 16°C). Although no chemical analysis was available it is presumed that the acids were essentially the straight chain form, or the normal acids. Unfortunately it was not possible to study the wave structure for all four acids since the concentrations used for heptanoic and octanoic acid led to sufficiently large stabilizing effects so that waves never appeared in the top 11 cm. of the film. Figure 4 shows experimental values of the distance from the top of the column at which waves are first visible vs. the Reynolds number; the concentrations listed are in moles per liter. These curves indicate a phenomenon which is quite similar to that which would be observed if a true critical Reynolds number existed, that is a Reynolds number below which the flow is stable to all disturbances. Under such circumstances the slope of the L vs. N_{Re} curve would become infinite at the critical Reynolds number. While the measurements obtained in this work do not indicate the existence of a true critical Reynolds number, the stability characteristics of the flow certainly indicate that a condition very similar to a critical Reynolds number does exist.

Previous theoretical work (*1, 4, 28, 29*) has shown that a critical Reynolds number does indeed exist for insoluble surface films, and is given by

$$N_{Re,c} = 1.68\left\{\frac{\left(\frac{\partial\sigma}{\partial\Gamma}\right)^3}{g\nu^4\rho^3\sin\theta}\right\}^{1/5} \tag{6}$$

where θ is the angle between the direction of flow and the gravity vector. Previous work (*28, 29*) also indicated that soluble surfactants could reduce the growth rate of waves to such an extent that a pseudo critical Reynolds number (32) might well be a reasonable parameter to

Table 1. Surface Elasticities and Elasticity Numbers Obtained from Pseudo Critical Reynolds Number and Equation 6

Solutions	$N_{Re,c}$	$(\partial\sigma/\partial\Gamma)$, dynes	N_{EL}
water	8	0.25	17
8.7×10^{-4} molar valeric acid	15	0.71	48
3.0×10^{-3} molar valeric acid	20	1.1	78
1.6×10^{-3} molar hexanoic acid	23	1.4	98
2.2×10^{-3} molar hexanoic acid	27	1.9	129
6.2×10^{-4} molar heptanoic acid	30	2.3	155
3.6×10^{-3} molar heptanoic acid	43	4.1	283

use in describing the flow characteristics of a falling liquid film. Because of the enormous computational difficulties, the analysis of the stability characteristics for a soluble surface film have not yet been extended to the point where we could properly interpret the curves shown in Figure 4; however, if we argue that the dominant effect of variations in the surface stress is not greatly effected by the interfacial mass transfer (that is it depends primarily on the rate of strain in the surface) we could use Equation (6) to determine the surface elasticity, $-\partial\sigma/\partial\Gamma$. This has been done and the results are shown in Table 1. The elasticity number N_{EL} shown in Table 1 is defined by

$$N_{EL} = \left(-\frac{\partial\sigma}{\partial\Gamma}\right)\left(\frac{2}{g\nu^4\rho^3}\right)^{1/3} \qquad (7)$$

and is a key parameter in both the stability analysis and the analysis of the entrance region flow.

In Figure 5 the measured wave numbers for four surfactant solutions are compared with a curve for pure water* based on both the theoretical and experimental results given in Figure 2. In Figure 5 we see that there is no significant effect of surface active agents on the wave number; a finding in agreement with previous investigators (*26*).

No data are presented for heptanoic or octanoic acid solutions for waves were not measureable (or observable) in the first 11 cm. of the top of the column for the solutions studied. In the case of octanoic acid, no waves appeared anywhere in the column for concentrations greater than 8×10^{-5} molar and Reynolds numbers as large as 200.

Previous calculations (*28*) indicate an upper bound for the critical Reynolds number resulting from surface elasticity effects should be 200, thus the absence of waves for the octanoic acid solutions can most likely be attributed to wave growth rates so small that waves were not visible in the 60 cm. column used in this work.

While the presence of surface active agents gives rise to no noticeable effect on the wave number, the effect on the wave velocity is quite another story. The experimental values of C_r are compared with a curve for pure water in Figure 6. Here we see that the wave velocity is drastically decreased for an increased surface elasticity.† It may be helpful at this point to review the theoretical predictions for the effect of surface elasticity on the wave velocity. The only calculations available (*28*) are for the special case of zero surface tension; nevertheless, these results should be helpful. Calculated values of the dimensionless wave velocity as a function of the Reynolds number are

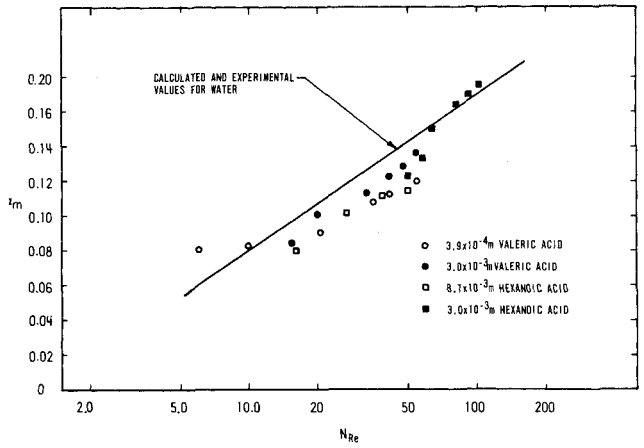

Fig. 5. Wave number having maximum growth rate vs. Reynolds number.

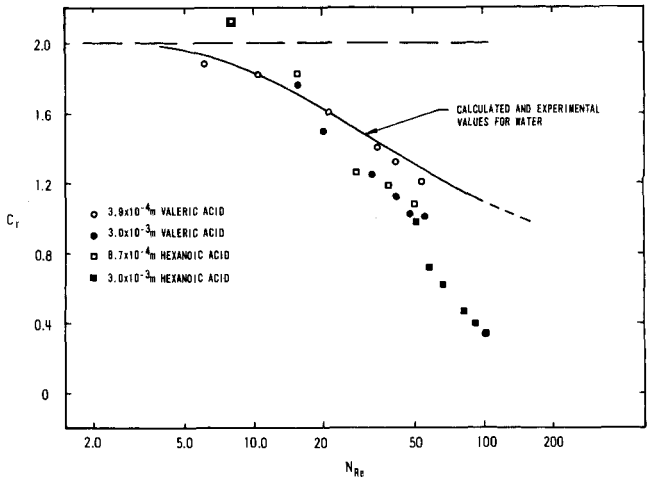

Fig. 6. Effect of surface active agents on wave velocity.

shown in Figure 7 for several values of the elasticity number. Here we see that increased values of the elasticity lead to increased values of the wave velocity rather than to the decreased values observed experimentally. Furthermore the measured values of C_r are as low as 0.40 indicating that the waves travel at a speed equal to 40% of the free surface velocity, u_o. This is in contrast to the theoretical calculations which indicate that u_o is a lower bound for the wave velocity (that is $C_r \geqq 1.0$).

The first thought that comes to mind at this point is that the surface velocity is greatly retarded by the presence of the surfactants. In effect, the adsorbed surface active agents form an elastic skin on the surface of the fluid and this retards the rapid acceleration that normally takes place at the top of the film.

FLOW IN THE ENTRANCE REGION

The steady, two dimensional flow in the entrance region illustrated in Figure 8 is governed by the equations of motion,

$$\rho\left(u\frac{\partial u}{\partial x} + v\frac{\partial u}{\partial y}\right) = -\left(\frac{\partial p}{\partial x}\right) + \rho g + \mu\left(\frac{\partial^2 u}{\partial x^2} + \frac{\partial^2 u}{\partial y^2}\right) \qquad (8a)$$

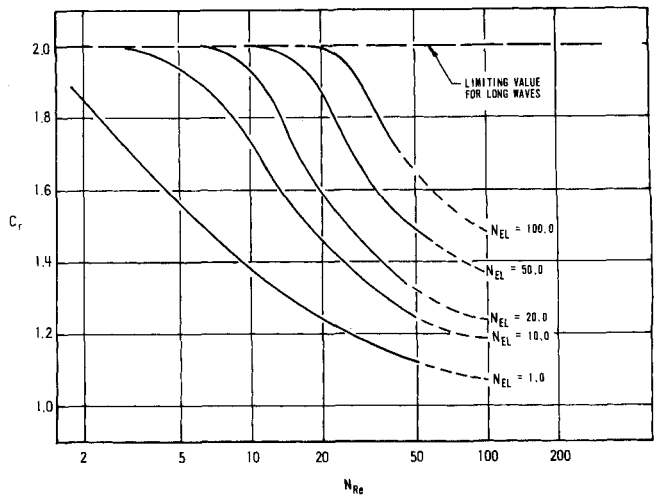

Fig. 7. Wave velocity for most unstable wave vs. Reynolds number ($N_\sigma = 0$).

* The words pure water refer to distilled water available in the laboratory. Care was taken to prevent contamination by surfactants, but the existence of a truly clean water surface is doubtful.

† We presume here at $-\partial\sigma/\partial\Gamma$ increases both with chain length and concentration for the low (that is much less than the critical micelle concentration) bulk concentrations studied in this work.

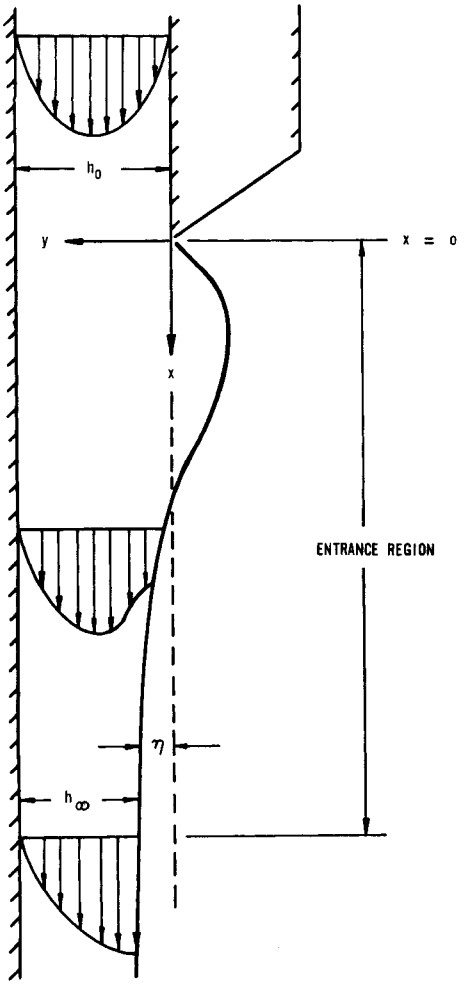

Fig. 8. Flow in the entrance region.

$$\rho\left(u\frac{\partial v}{\partial x}+v\frac{\partial v}{\partial y}\right)=-\left(\frac{\partial p}{\partial y}\right)+\mu\left(\frac{\partial^2 v}{\partial x^2}+\frac{\partial^2 v}{\partial y^2}\right) \tag{8b}$$

the continuity equation

$$\frac{\partial u}{\partial x}+\frac{\partial v}{\partial y}=0 \tag{9}$$

and the diffusion equation.

$$u\left(\frac{\partial c}{\partial x}\right)+v\left(\frac{\partial c}{\partial y}\right)=\mathcal{D}\left(\frac{\partial^2 c}{\partial x^2}+\frac{\partial^2 c}{\partial y^2}\right) \tag{10}$$

A complete solution for the entrance region flow presents a formidable computational problem primarily because of the difficulties associated with locating the interface and imposing the proper surface boundary conditions.

If we impose the restriction that the liquid film depth is constant and that $v = 0$ everywhere, the analysis is greatly simplified at the cost of violating the continuity equation. In making this step we are abandoning the idea of obtaining a close approximation to the real flow field, while retaining the hope that the solution will properly indicate the effect of surface elasticity on the entrance region flow field. Under these circumstances the governing equations and boundary conditions (in dimensionless form) reduce to‡

$$U\frac{\partial C}{\partial X}=2+\left(\frac{\partial^2 U}{\partial Y^2}\right) \tag{11}$$

$$U\frac{\partial C}{\partial X}=\frac{1}{N_{Sc}}\left(\frac{\partial^2 C}{\partial Y^2}\right) \tag{12}$$

boundary condition 1*a*

$$U=4(Y-Y^2),\quad X=0 \tag{13a}$$

boundary condition 1*b*

$$C=1,\quad 1\geqq Y>0,\quad X=0 \tag{13a}$$

boundary condition 1*c*

$$C=0,\quad Y=0,\quad X=0 \tag{13c}$$

Note that a singularity appears in the concentration at $X = Y = 0$. This occurs because the dimensionless surface concentration Γ must be zero at $X = Y = 0$.

boundary condition 2

$$U=\frac{\partial C}{\partial Y}=0,\quad Y=1 \tag{14}$$

boundary condition 3

$$\frac{\partial}{\partial X}(UC)=(KN_{Sc})^{-1}\left(\frac{\partial C}{\partial Y}\right),\quad Y=0 \tag{15}$$

boundary condition 4

$$\Gamma=C,\quad Y=0 \tag{16}$$

boundary condition 5

$$\left(\frac{\partial U}{\partial Y}\right)=N_{EL}\,N_{Re}^{-2/3}\left(\frac{\partial \Gamma}{\partial X}\right),\quad Y=0 \tag{17}$$

Equations (15) and (17) are derived from the surface mass and momentum balances and are described elsewhere (*29*).

METHOD OF SOLUTION

An explicit forward difference method [*11* (p. 92)] was used to solve Equations (11) and (12) subject to the boundary conditions given by Equations (13) to (17). If $N_{EL} = 0$ these equations are uncoupled and no iterative routine was needed. For nonzero values of N_{EL} the equations are coupled through Equations (15), (16), and (17) and one must assume values of U and C at $X + \Delta X$ and use these in conjunction with known values at X in order to compute new values at $X + \Delta X$. If the computed values of U and C are within some specified tolerance of the assumed values, the iterative process has converged and new step is taken in the X direction. In practice the solution has converged when successive calculations of the entire U and C fields show no appreciable change for a decrease in the tolerance, and a decrease in the mesh size.

One of the difficulties encountered in solving Equations (11) and (12) is that for the uncoupled case, the characteristic length in the X direction is on the order of unity for the momentum equation, whereas the characteristic length in the X direction is of the order of N_{Sc} for the diffusion equation. Because of this small values of ΔX are required if we are to obtain reasonable results for the U field; however, small values of ΔX present a problem in the solution of Equation (12). The set of finite difference equations resulting from Equation (12) can be solved by inverting the tridiagonal matrix of coefficients of the linear equations. However, the diagonal terms in that matrix are on the order of $N_{Sc}\Delta Y^2/\Delta X$ and large values of the diagonal terms lead to unstable behavior especially

‡ Here we have made the standard boundary layer assumption $\partial^2 u/\partial x^2 << \partial^2 u/\partial y^2$ and $\partial^2 C/\partial x^2 << \partial^2 C/\partial y^2$. This leads to parabolic differential equations and forces us to drop the viscous terms in the surface momentum balance.

for nonzero values of N_{EL}. This difficulty was overcome to some extent by using a variable mesh size in both the X and Y directions. In particular, small values of ΔY were used in the neighbor of $Y = 0$, for this is the region where the largest changes in both U and C took place.

The surface velocity profile for $N_{EL} = 0$ is compared with the experimental data of Lynn (*18*) in Figure 9. Here we see that the calculated surface velocity is as much as 20% below the experimental values which were obtained for three different Reynolds numbers. The case where $N_{Re} = 970$ is the only experimental condition where $h_0 = h_\infty$, thus it is this set of data which should show the best agreement with the calculated values. While the lack of agreement is not particularly encouraging, it is not surprising to find such large differences when we consider the extreme simplification that was imposed upon the complete equations in order to obtain Equations (11) and (12). If one were to use this method to determine entrance lengths (that is the distance required for the velocity to approach 99% of the final velocity) the error would be intolerable; however, if one simply wants a reasonable estimate of the velocity, the method appears to give values within 20% of the real values. Furthermore, it is expected that the comparison with experimental results for pure water probably represents the severest test of the analysis, for it is under these circumstance that the variations of U and V with x are the largest. When surface active agents are present and the acceleration of the free surface is retarded, we can expect smaller values of v and $\partial^2 u/\partial x^2$ thus the simplifying assumptions become more palatable.

In Figure 10, calculated surface velocity profiles are shown for $N_{EL} = 0$, 1, 3, and 170; the largest value being the value for 3.0×10^{-3} molar hexanoic acid estimated from the curves shown in Figure 4 and Equation (6). In Figure 10 we see that our initial suspicion regarding the retarded surface velocities is confirmed. Note that for a Reynolds number of 100, a uniform flow is not reached for about 50 cm. in contrast to an entrance length of less than 1 cm. for pure water. Even though the calculations are only an approximation, there is no question that uniform flow is extremely difficult to obtain in a wetted wall column if appreciable amounts of surfactant are present. It should be kept in mind that valeric and hexanoic acid are rather mild stabilizing agents, and it is not hard to imagine that small amounts of octanoic acid would produce surface velocities perhaps an order of magnitude smaller than u_o over distance on the order of 50 cm. This finding requires that mass transfer data obtained in wetted wall columns stabilized with surfactants (*9, 17, 27*) must be considered with caution. On one hand, surfactants would reduce mass transfer rates owing to the reduction of wave motion (*25*) and owing to the increase in interfacial resistance (*30*), while on the other hand the overall mass transfer rate would be substantially increased owing to the increased contact time. The results presented here raise some doubt about the use of Equation (6), in conjunction with the experimental data shown in Figure 4, to calculate the surface elasticity. Equation (6) results from the stability analysis of a uniform flow (that is v_x, c, and γ independent of x) whereas the data shown in Figure 4 were taken under conditions such that both the velocity and surface concentration were changing in the direction of flow. Because of this, the elasticity numbers listed in Table 1 must be considered as rough estimates. A great deal of analysis must be done before reliable values of the surface elasticity can be extracted from curves such as those shown in Figure 4.

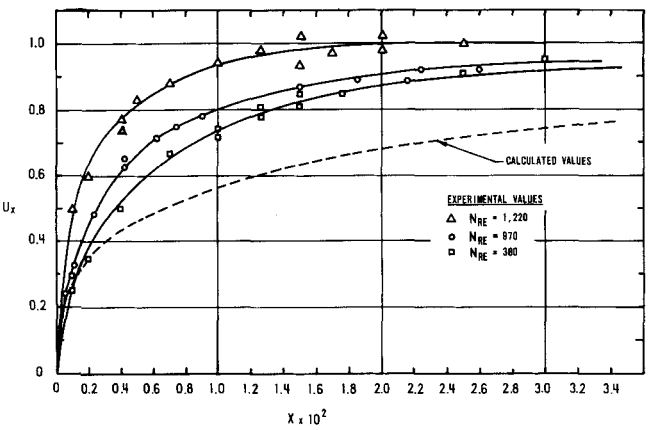

Fig. 9. Surface velocity in the entrance region of a falling liquid film.

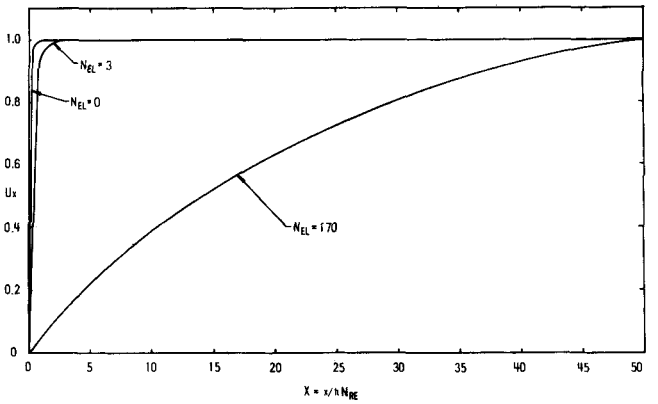

Fig. 10. Calculated surface velocity in the entrance region of a falling film for $N_{Re} = 100$.

In a final effort to confirm the postulated mechanism for the observed low wave velocities, we can use the calculated surface velocity in conjunction with previous stability studies to estimate the wave velocities for a 3.0×10^{-3} molar hexanoic acid solution. In order to do this, the results shown in Figure 10 for $N_{EL} = 170$ and $N_{Re} = 100$ were extended to provide surface velocity profiles for Reynolds numbers of 50 and 20 at the same elasticity number, $N_{EL} = 170$. These results allowed us to estimate the surface velocity at a point 11 cm. from the top of the film as a function of the Reynolds number. If we assume that previous calculations (28) of (c_r/u_o) for uniform flow are actually equal to $(c_r/u|_{y=0})$ for the flows studied experimentally we can write[§]

$$(c_r/u_o)_{\text{calc}} = (c_r/u|_{y=0})_{\text{meas}} \tag{18}$$

which may be expressed as

$$(C_r)_{\text{calc}} = \left(\frac{c_r}{u_o}\right)_{\text{meas}} \left(\frac{u_o}{u|_{y=0}}\right)_{\text{calc}} \tag{19}$$

Now, $(C_r)_{\text{calc}}$ is the value of C_r shown in Figure 6 and $(u|_{y=0}/u_o)$ is the dimensionless velocity determined by Equation (11) and shown in Figure 10 for the special case, $N_{Re} = 100$. We can estimate the measured values of the dimensionless wave velocity by the expression

$$(C_r)_{\text{meas}} = (C_r)_{\text{calc}}\, U_{\text{calc}} \tag{20}$$

Values of $(C_r)_{\text{calc}}\, U_{\text{calc}}$ are plotted in Figure 11 along with the experimental values for 3.0×10^{-3} molar hexanoic acid. The good agreement between the analysis and the experimental data is to some extent fortuitous, but in any event it confirms our suspicions regarding the nature of the flow.

§ This assumption is encouraged by the excellent results obtained by Anshus and Goren (*2*) which indicated that the stability of the flow depends primarily on the free surface velocity.

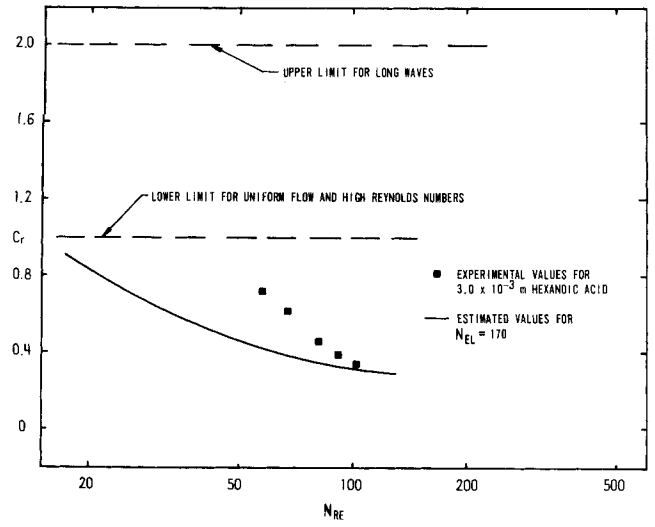

Fig. 11. Comparison of experimental and estimated values of the wave velocity in the entrance region.

CONCLUSIONS

The experiments described in this paper have confirmed previous observations (26) that the addition of surfactants to falling liquid films does not appreciably alter the wave length of the waves that appear when the film becomes unstable. Furthermore, it has been shown that the study of wave velocities for such flows is a difficult task because of the very long columns which must be used if uniform flow is to be obtained.

Of importance is that the onset of waves occurs in a manner quite suggestive of a critical Reynolds number phenomena, and that a pseudo critical Reynolds number can be used to estimate the thermodynamic quantity, $-\partial\sigma/\partial\Gamma$. Furthermore, these experiments have indicated that the entrance region is greatly increased when surfactants are present. Measurements of the surface velocity in the entrance region can also be used to explore the process of mass transfer of surfactants to the gas-liquid interface and to confirm values of the elasticity obtained by the pseudo critical Reynolds number measurements.

ACKNOWLEDGMENT

This work was supported by the U.S. Army Research Office, Durham.

NOTATION

c = bulk phase mass density of surfactant, g. cm.$^{-3}$
c_o = initial mass density of surfactant, g. cm.$^{-3}$
C = c/c_o, dimensionless mass density of surfactant
c_r = wave velocity, cm. sec.$^{-1}$
C_r = c_r/u_o, dimensionless wave velocity
$\mathcal{D}$ = bulk phase diffusion coefficient, sq. cm. sec.$^{-1}$
g = gravitational acceleration, cm. sec.$^{-2}$
h = fluid depth, cm.
h_o = fluid depth at $x = 0$, cm.
h_∞ = uniform fluid depth ($x \to \infty$), cm.
K = equilibrium coefficient, cm.
$\mathcal{K}$ = K/h_∞, dimensionless equilibrium coefficient
m = moles per liter
p = fluid pressure, dynes cm.$^{-2}$
p_o = ambient pressure, dynes cm.$^{-2}$
u_o = free surface velocity for uniform flow, cm. sec.$^{-1}$
u, v = scalar components of the bulk phase velocity vector in the x and y directions respectively, cm. sec.$^{-1}$
U, V = u/u_o, vN_{Re}/u_o, dimensionless scalar components of the velocity vector
x, y = rectangular Cartesian coordinates, cm.
X, Y = $x/N_{Re}\ h_\infty$, y/h_∞, dimensionless rectangular coordinates

Greek Letters

α = $2\pi h/\lambda$, dimensionless wave number
γ = surface mass density, g. cm.$^{-2}$
γ_o = $K\ c_o$, g. cm.$^{-2}$
Γ = γ/γ_o, dimensionless surface mass density
η = $h_o - h$, position of the interface, cm.
λ = wave length, cm.
μ = bulk fluid viscosity coefficient, dyne-sec.-sq.cm
ν = μ/ρ, kinematic viscosity coefficient, sq. cm. sec.$^{-1}$
ρ = fluid density, g. cm.$^{-3}$

Dimensionless Numbers

N_{EL} = $(-\partial\sigma/\partial\Gamma)\ (2/g\nu^4\rho^3)^{1/3}$, elasticity number
N_{Re} = $(u_o h_\infty/\nu)$, Reynolds number
$N_{Re,c}$ = critical Reynolds number
N_{Sc} = $\nu/\mathcal{D}$, Schmidt number

LITERATURE CITED

1. Anshus, B. E., and Andreas Acrivos, *Chem. Engr. Sci.*, **22**, 2389 (1967).
2. Anshus, B. E., and S. L. Goren, *AIChE J.*, **12**, 1004 (1966).
3. Bede, The Venerable, "Ecclesiastical History" Book III, Chapt. 14, London, Bell, and Daldy, London, England (1871).
4. Benjamin, T. B., *Arch. Mech. Stos.*, **16**, 615 (1964).
5. Berg, J. C., and Andreas Acrivos, *Chem. Engr. Sci.*, **20**, 737 (1965).
6. Bromley, L. A., R. F. Humphreys, and W. Murray, *Trans. Am. Soc. Mech. Eng., Ser. C.*, **88**, 80 (1966).
7. Bruley, D. F., *AIChE J.*, **11**, 945 (1965).
8. Davies, J. T., and E. K. Rideal, "Interfacial Phenomena," Academic Press, New York (1963).
9. DeNevers, Noel, *AIChE J.*, **12**, 1110 (1960).
10. Farley, R. W., and R. S. Schechter, *Chem. Engr. Sci.*, **21**, 1079 (1966).
11. Forsythe, G. E., and W. R. Wasow, "Finite-Difference Methods for Partial Differential Equations," John Wiley, New York (1960).
12. Hansen, R. S., *J. Colloid Sci.*, **16**, 549 (1961).
13. Jones, L. O., MS thesis, Northwestern Univ., (1965).
14. Jones, L. O., and Stephen Whitaker, *AIChE J.*, **12**, 525 (1966).
15. Knuth, E. L., *Jet Propulsion*, **24**, 359 (1954).
16. Levich, V. G., "Physicochemical Hydrodynamics," Prentice-Hall, Englewood Cliffs, N.J. (1962).
17. Lynn, S., et. al., *Chem. Eng. Sci.*, **1**, 40 (1955).
18. Lynn, Scott, *AIChE J.*, **6**, 703 (1960).
19. Paris, Jean, and Stephen Whitaker, *ibid.*, **11**, 1033 (1965).
20. Schlichting, Hermann, "Boundary-Layer Theory," McGraw-Hill, New York (1955).
21. Scriven, L. E., and C. V. Sternling, *AIChE J.*, **5**, 514 (1959).
22. Sinha, Vinod, Ph.D. thesis, Univ. California, Davis (Dec. 1967).
23. Slattery, J. C., *Ind. Eng. Chem. Fundamentals Quart.*, **6**, 108 (1967).
24. Sterba, C., and D. M. Hurt, *AIChE J.*, **1**, 178 (1955).
25. Tailby, S. R., and S. Portalski, *Trans. Inst. Chem. Engrs.*, **38**, 324 (1960).
26. *Ibid.*, **40**, 114 (1962).
27. Ternovskaya, A. N., and A. P. Belopol' skii, *Zhur. Fiz. Khim.*, **24**, 43, 981 (1950).
28. Whitaker, Stephen, *Ind. Eng. Chem. Fundamentals Quart.*, **3**, 132 (1964).
29. ——— and L. O. Jones, *AIChE J.*, **12**, 421 (1966).
30. ——— and R. L. Pigford, *ibid.*, **12**, 741 (1966).
31. Zotikov, I. A., and L. N. Bronskii, *Inzh. Fiz. Zhur. Akad. Nkad. Nauk Belorussk*, **5**, 10 (1962).
32. Benjamin, T. B., *J. Fluid Mech.*, **2**, 554 (1957).

Manuscript received January 2, 1968; revision received April 18, 1968; paper accepted April 19, 1968.